The formation mechanism of multilayer emulsions studied by isothermal titration calorimetry and dynamic light scattering

Wei Liao, Emilie Dumas, Abdelhamid Elaissari, Adem Gharsallaoui

A study of the formation mechanism of multilayer emulsions by isothermal titration calorimetry and dynamic light scattering

Wei Liao[1], Emilie Dumas[1], Abdelhamid Elaissari[2], Adem Gharsallaoui[1]*

[1] Univ. Lyon, University Claude Bernard Lyon 1, CNRS, LAGEPP UMR 5007, 43 Bd 11 Novembre 1918, 69622 Villeurbanne, France

[2] Univ Lyon, University Claude Bernard Lyon 1, CNRS, ISA-UMR 5280, 69622 Villeurbanne, France

*Corresponding author: adem.gharsallaoui@univ-lyon1.fr

Abstract

The formation of multilayered interfaces around oil droplets in oil-in-water (O/W) systems has great advantages in delivering lipid-soluble active compounds. Until now, few thermodynamic analyses have been performed on the preparation process of multi-layer emulsions. In this study, isothermal titration calorimetry (ITC) and dynamic light scattering (DLS) were used to investigate the binding properties and physical properties of low methoxyl pectin (LMP) and sodium caseinate (CAS) based multilayer emulsions during the formation process. ITC titration confirmed LMP does bind CAS-coated droplets through the electrostatic forces and it was a spontaneous exothermic process ($\Delta G < 0$, $\Delta H < 0$). Furthermore, stable multilayer emulsions can be only formulated by titrating the primary emulsion into LMP instead of back-titrating. Finally, the effects of different mixing methods on the stability of multilayer emulsions were evaluated. The DLS results suggest that titration rather than mixing directly can lead to more uniform and smaller-sized droplets, which can be attributed to the fact that slow titration can effectively avoid droplet aggregation.

Keywords: Multilayer emulsions; Isothermal titration calorimetry; Dynamic light scattering; Electrostatic interactions; Bridging flocculation

1. Introduction

Oil in water (O/W) emulsion systems, produced by homogenizing oil and aqueous phases together in the presence of one or more emulsifiers, have been extensively applied in foods such as soft drinks, milk, mayonnaise, and vinaigrette, etc. (Guzey & McClements, 2006). Along with the food safety concerns, there is a growing interest trend in the food field to replace commercial synthetic emulsifiers with natural "label-friendly" ones (Dammak et al., 2020). In this regard, several food protein-based emulsifiers, from different sources like milk, whey, eggs, legume, oilseed, and so on, have been extensively investigated as natural emulsifiers in recent years due to their amphiphilic character, polymeric structure, and electrical charge characteristics (Kim et al., 2020). Despite their favorable properties, protein-stabilized emulsions have been reported to be highly sensitive to environmental stresses such as pH, ionic strength, temperature, and oxygen (Bouyer et al., 2012). This instability of protein-based emulsions under these conditions will limit their further application in certain commercial products. In fact, the quality and stability of emulsions can be improved by combining protein emulsifiers with other natural polymers to form multilayered interfaces (Surh et al., 2006). For example, protein-coated droplets are either negatively or positively charged when the pH is below or above their isoelectric point (pI) (Wang et al., 2019), and then they could attract the oppositely charged polysaccharides present in the continuous phase, thereby forming a thicker layer at O/W interface. Zhang et al. (2020) developed multilayer emulsions by addition of camellia saponin (CS) into almond protein isolate (API) based primary emulsions at pH 3. Compared with primary emulsions, droplets with multi-layered interfaces have the ability to significantly inhibit lipid and protein oxidation during storage. Compare with emulsions with single-layer interfaces, emulsions with multilayered interfaces were also found to have better stability against environmental stresses, such as pH extremes, high ionic strengths, thermal processing, and freezing (Ogawa et al., 2003, 2004).

The basic mechanism for the preparation of multilayer interfaces is by adding oppositely charged polymers to a "primary" emulsion prepared by conventional

homogenization techniques (Ogawa et al., 2003). As a result, a "secondary" emulsion with a two-layer interface could be formulated due to electrostatic attraction. This process can be repeated several times to produce three or more-layer emulsions with desired functional properties. Previous studies (Guzey & McClements, 2006; McClements, 2012) demonstrated that adsorption layers can be deposited around droplets in two different ways: a one-step or two-step mixing procedure, depending on the charge-pH properties of the used biopolymer. In the one-step mixing method, a solution containing oppositely charged biopolymers is directly mixed with a primary emulsion containing charged droplets. This approach tends to promote the tendency of droplets to flocculate or coalesce during the process, and the aggregation is generally irreversible (Guzey & McClements, 2006; Surh et al., 2006). In the two-step method, the solution containing the charged biopolymer is mixed with the primary emulsion at a pH where there is no strong electrostatic attraction between them. The pH of the mixture is then adjusted to a pH where the droplets and the unabsorbed polymer have opposite charges, so that the polymer can be adsorbed to the droplet surface. This method is usually preferred for the production of multilayered interfaces at laboratory scale, since the second layer of biopolymer is more uniformly distributed throughout the aqueous phase prior to adsorption (Liu et al., 2022; Mundo et al., 2021; Shi et al., 2021). Nonetheless, the two-step approach has several drawbacks: (i) Irreversible aggregation occurs when the pH is adjusted to pass the pI of the protein emulsifier; (ii) not suitable for the preparation of emulsions with more than two layers; (iii) relatively complex process is not suitable for industrial mass production. For this reason, the one-step approach was selected in our study and further optimized to avoid droplet aggregation for preparing stable multilayer emulsions.

To minimize droplet aggregation in the one step method, it is necessary to ensure that enough biopolymers for coatings is present in the system to surround the entire surface of the added oil droplets. Otherwise, bridging flocculation may occur, as one polyelectrolyte may adsorb to the surface of multiple droplets, causing them to link together (McClements, 2012). Even with sufficient free polyelectrolyte concentration in the aqueous phase, droplet aggregation cannot be completely avoided because

particle-particle collisions are sometimes faster than the adsorption of biopolymers to the surface of the primary coating droplets. One strategy to avoid the droplet aggregation during the process of forming multilayer emulsions is to control the ratio of mixing by titrating primary emulsions into coating solutions (Zeeb et al., 2015). Therefore, the concentration and mixing methods of biopolymers must be carefully designed to avoid extensive droplet aggregation and massive free polyelectrolyte remaining in the aqueous phase after the coating step.

The saturation concentration for a mutilayer system has been mostly characterized by dynamic light scattering (DLS), which provides the saturation condition by identifying the ζ-potential plateau (Okubo & Suda, 2003). In this study, we used isothermal titration calorimetry (ITC) and conventional DLS to investigate the interaction and thermodynamic characteristics between sodium caseinate (CAS) stabilized emulsion and low methoxyl pectin (LMP) during the preparation of multilayer emulsions. In the first part, the thermodynamic parameters and surface charge during the formation (titration and back-titration) of the multilayer emulsion were evaluated to understand the stabilization mechanism of the multilayer emulsion during the preparation. Meanwhile, the advantages of ITC and DLS in measuring the system are described and compared. In the second part, the multilayer emulsions prepared by titration and direct mixing methods were compared in terms of particle size distribution, zeta potential (ζ-potential), creaming behavior, microstructure, and fluorescence intensity. This research could provide more information for the rational design of multilayer emulsions.

2. Materials and methods

2.1. Materials

The powder of CAS with 93.20% protein content (determined by the Kjeldahl method, N=6.38) was purchased from Fisher Scientific (UK). The powder of LMP (esterification degree from 22% to 28% and acetylation degree from 20% to 23%) with 81.21% carbohydrate content was obtained from Cargill (Baupte, France). A medium chain triacylglycerol oil (MCT) was purchased from Gattefossé (Saint-Priest,

France). Imidazole, acetic acid, sodium azide, sodium hydroxide, and hydrochloric acid were purchased from Sigma-Aldrich Chimie (St Quentin Fallavier, France). The water used in all preparations was deionized water.

2.2. Sample preparation

Imidazole-acetate buffer solutions (5 mM) containing 0.04 wt.% sodium azide (to avoid microbial growth, (Chang et al., 2016)) was prepared by dispersing weighed amounts of imidazole and acetic acid into deionized water. Biopolymer stock solutions were prepared by slowly dispersing 0.53 wt.% CAS and 0.50 wt.% LMP separately into 5 mM imidazole-acetate buffer and stirring overnight to ensure complete hydration. The pH of both stock solutions was then adjusted to 3.0 by adding HCl (1 M) 24 h prior their use.

2.3. Preparation of primary emulsions and multilayer emulsions

Oil-in-water coarse emulsions were prepared by mixing 5.0 g MCT oil and 95 g emulsifier aqueous solution (0.53 wt.% CAS stock solution at pH 3.0) by high-speed homogenization (IKA, Staufen, Germany) under 13,500 rpm for 5 minutes. The resultant pre-emulsions was then passed through a microfluidizer (Microfluidics LM20, Microfluidics Corp., Newton, MA, USA) 5 times at 5×10^7 Pa to obtain nanoemulsions (Liao et al., 2021). The obtained nanoemulsions (containing 0.5 wt.% CAS) were then adjusted to pH 3.0 and considered as “primary emulsions”.

Multilayer emulsions were prepared by titrating the primary emulsions into LMP stock solution (0.5 wt.%) at a rate of 2.5 mL/min by using an automated procedure with the TitroLine 5000 (TitroLine 5000, Xylem Analytics GmbH, Weilheim in Oberbayern, Germany). During the titration, the samples were kept under agitation and different ratios of primary emulsion/LMP were collected for subsequent analysis. To investigate the effect of LMP on the formulation of multilayer emulsions when the coating material was insufficient, back-titration was also performed on the same ratio of CAS-based emulsion/LMP. Meanwhile, direct mixing was performed by slowly pouring different volumes of primary emulsions in same ratios (w/w) into the LMP stock solution under stirring to compare the effects of different mixing methods on the multilayer emulsions.

2.4. Isothermal titration calorimetry (ITC)

The energetics of the interactions between primary emulsions and LMP was measured using an isothermal titration calorimeter (VP-ITC) from MicroCal (Malvern Instruments, Northampton, MA) in a reaction cell volume of 1.4214 mL. LMP and CAS-based emulsions were diluted to the desired concentration (0.05 or 0.50 wt.%) with the same buffer (5 mM imidazole-acetate buffer, pH 3.0). All solutions were degassed under stirring for 5–10 min before being loaded. The pH of each solution was checked again before measuring to ensure the same values in the cell and in the syringe. The calorimetric cell was filled with LMP solution (0.5 wt.%) and the electric injector was filled with CAS-based emulsion (0.05 wt.%), equilibrated at 25 °C. The titration was performed by adding an initial 2 μL injection and 28 consecutive 10 μL injections while continuously stirring the mixture at 307 rpm. Each injection lasted 20 s with a 200 s interval between consecutive injections. Back-titration was also performed by placing the CAS-based emulsion (0.5 wt.%) into the cell and the LMP solution (0.05 wt.%) into the syringe, separately. Controlled titrations were performed by injecting the primary emulsion or LMP solution into imidazole-acetate buffer to obtain the heat of dilution, so corrected data were obtained by subtracting the heat of dilution data from the raw data. Data analysis was carried out by Origin 7.0 software. The Gibbs free energy is calculated by the equation $\Delta G=\Delta H - T\Delta S$. Measurements were performed in triplicate and results are reported as mean and standard deviation.

2.5. Intrinsic fluorescence

Intrinsic fluorescence intensity of multilayer emulsions with different ratios of CAS-based emulsion/LMP was carried out at room temperature by a multimode microplate reader equipped with a temperature-controlled 96-wells microplate (Thermo Scientific™ Varioskan). The excitation wavelength was set at 280 nm and the emission spectrum was recorded in the wavelength range of 298-550 nm with an excitation and emission slit width of 5 nm. The multilayer emulsions formulated by titration in different ratios was diluted with 5 mM imidazole acetate buffer (pH 3.0) to a final concentration of 0.05 wt.% CAS. The diluted samples were then evenly transferred to 96-well plates for analysis, with 6 measurements per sample. The

fluorescence intensity of acetate-imidazole buffer and pure LMP solution were used as a blank and a control, separately.

2.6. Zeta potential (ζ potential)

The ζ potential was performed by electrophoretic mobility (Malvern Instruments, Worcestershire, UK) under room temperature. To avoid multiple scattering effects, each sample was diluted to a concentration of around 0.05 wt.% with the same buffer (5 mM imidazole-acetate buffer, pH 3). Diluted samples were transferred to disposable cells for electrophoretic mobility measurement. All measurements were performed three times and the ζ-potential values were calculated by the software as the average of three individual measurements.

2.7. Mean particle size

Mean particle size (nm), polydispersity index (PdI) and size distribution were determined by dynamic light scattering using a Zetasizer Nano-ZS90 (Malvern Instruments, Worcestershire, UK) under room temperature. To eliminate multiple scattering effects, each sample was diluted to a droplet concentration around 0.1 wt.% with corresponding pH buffers. After 90 s of equilibrium, each sample was analyzed three times.

2.8. Microscopic image

Before analysis, each sample should be gently stirred in glass tubes to ensure they were homogeneous. A drop of the emulsion was placed on a microscope slide and covered with a coverslip. The microstructure of samples was then visualized at room temperature using an Evos bright-field microscope (EVOS M5000, Thermo-Invitrogen, USA).

2.9. Statistical analysis

All experiments were carried out at least three times with freshly prepared samples. Data are reported as means ± standard deviations.

3. Results and discussions

3.1. Formation mechanism of multilayer emulsions

3.1.1. Zeta potential analysis

The appropriate concentration of the biopolymer coating around the primary emulsion can usually be assessed by measuring the zeta potential (Okubo & Suda, 2003). It has been reported that the ζ-potential of colloidal systems varies with the continuous addition of adsorbable polymers, and the plateau of the ζ-potential as function of ratio is related to the surface saturation of the polymer coating (Chang et al., 2016).

Fig. 1 showed the ζ-potential of multilayer emulsions prepared by titration and back-titration as function of CAS/LMP or LMP/CAS ratio. The ζ-potential of pure LMP solution (Fig.1A) at pH 3.0 is negative (-17.0 mV) which is attributed to the ionization of its carboxyl groups. When the ratio of CAS-based emulsion/LMP is increased, the ζ-potential initially remain stable until the ratio reached 0.5, then became increasingly less negative, with a point of zero charge in the ratio range around 1.25 - 1.50, and finally reached a plateau for higher ratio (3.0) (ζ-potential close to that of primary emulsion). This is the fact that the primary emulsion exhibited positive charge at pH 3.0 because the protonation of the basic side chain (NH_3^+) of the casein molecule. As a result, LMP molecules can be adsorbed on the droplet surface by electrostatic force, and then the overall negative charge of the system gradually increases until there are not enough LMPs in the system to cover the newly dropped droplet. As shown in Fig. 1B, the ζ-potential of the primary emulsion is positive (+32.6 mV) and this value could be considered enough to ensure high intermolecular repulsions (Lieberman et al., 2020). When the LMP concentration was increased, the ζ-potential initially remains stable until the ratio reaches 0.3, then becomes increasingly less positive, with a point of zero charge in the ratio range around 0.6 - 0.8, and finally reached a plateau at a ratio of 1.5 (Fig.1B). According to previous reports (Chang et al., 2016; Liu et al., 2019), the plateau of ζ-potential indicates that the lipid droplet surface is saturated with coating polysaccharides at this level. It should be mentioned that during the experiment, the titration of the primary emulsion

into the LMP solution resulted in a stable multilayer emulsion, while titration in the opposite direction (LMP solution into the primary emulsion) showed obvious flocs and these flocs did not disappear with the continuous addition of LMP (Data not shown). Based on our results, the forward titration reached a plateau at a ratio 3.0 (Fig. 1A), which corresponds exactly to a ratio of 0.3 (Fig. 1B) for titration of the primary emulsion into the LMP solution. After the ratio 0.3, the absolute value of the zeta potential begins to decrease, indicating that the droplet saturation potentials corresponding to the titrated and back-titrated samples are consistent. Therefore, this finding suggests that the zeta potential can represent the overall distribution of particles in solution but cannot reflect whether the multilayer emulsion formulation is stable during preparation (the occurrence of particle aggregation).

Meanwhile, to find the exact concentration of coating polymer at which the multilayer emulsions reach the plateau, a large number of samples in different ratios should be prepared to measure for ζ-potential measurements, which are considered very complex and time-consuming processes. In this regard, we employed ITC to measure thermodynamic parameters to gain a deeper understanding of the stoichiometry of layer-by-layer interactions and to analyze the energetics of multilayered interfaces processes.

3.1.2. ITC analysis

ITC have been widely used to investigate molecular interactions in biological systems (Jafari et al., 2007; Wang et al., 2019), but there are few reports on the interaction between droplets and molecules (Fotticchia et al., 2014). Hence, ITC was used to obtain more information about the evolution of deposition around the primary emulsion, such as the equilibrium adsorption constant, enthalpy of adsorption, and adsorption stoichiometry. CAS-based emulsions and LMP solutions at pH 3.0 were chosen to perform ITC tests at 25 °C because CAS-coated droplets showed positive charge and LMP molecules showed negative charges at pH 3.0 (Wang et al., 2019). In this study, heat flow versus time curves (the upper of Fig. 2) were obtained by gradually injecting 0.5 wt.% primary emulsion or 0.5 wt.% LMP solution into a reaction cell containing 0.05 g/L LMP solution or 0.05 wt.% primary emulsion at

25 °C. The enthalpy changes (the lower of Fig. 2) as function of mass ratio were obtained by the software. The mass unit was used to replace the molecular unit in this study, because both CAS and LMP are high molecular weight polymers.

The ITC measurements (Fig. 2A) showed that the titrating process was exothermic with a stepwise change in the exothermic value for each injection. When the ratio of primary emulsion/LMP is lower than 1.0, the values of heat released per injection are very close, which indicates that the injected CAS-coated droplets have a more stable interaction with the LMP molecules in the reaction cell at this stage. This phase also corresponds to that when the absolute value potential of zeta (Fig. 1A) gradually approaching the "0" point from larger values (-17.0 mV to -8.42 mV), implying that multiple emulsions may go from stable to relatively unstable from this point (Ratio 1.0). This was probably attributed to the fact that, at the initial stage, excess negative LMP molecules in the cell can quickly adsorb on the surface of the positively charged emulsion droplets due to electrostatic interactions. Our previous study (Wang et al., 2019) reported the interaction between CAS and LMP when used at the same contents in this study. Interestingly, the heat released by the interaction between CAS and LMP decreases with regularity from the beginning. This difference may stem from differences in binding between molecules and between molecules and droplets. The CAS-encapsulated droplets prepared in this study have nanoscale diameters with an average particle size of about 300 nm, so the CAS molecules adsorbed on the surface of the oil droplets have a more ordered structure in the system than free casein molecules in the aqueous phase. As a result, each casein-coated droplet entering the cell has enough LMP molecules to cover the droplet surface through electrostatic attraction rather than disordered droplet aggregation, thereby releasing a relatively stable heat per injection at the initial stage. For ITC measurements between CAS and LMP solutions, complexes were formed during each injection and these complexes were confirmed to be insoluble at pH 3.0 (Wang et al., 2019). Therefore, it can be hypothesized that the casein molecules may rapidly form disordered network fibers after entering the reaction cell, and the degree of network structure is more extensive, and the heat released is higher. When the ratio was above 1.0, the heat released per

injection stated to decrease regularly (Fig. 2A). This may be attributed to the gradual depletion of LMP chains in the reaction cell. Above the ratio of 1.4, the enthalpy becomes slightly positive and remains stable, indicating that none of the LMP molecules in the cell can interact with the newly added droplet. However, the result of zeta potential (Fig.1 A) showed that the plateau was obtained when the ratio of CAS-based emulsion/LMP was around 3.0, which was not consist with ITC results. It was reported that the ζ-potential is highly sensitive to the environmental conditions, and slight differences in the ion concentration can affect measurements (Fotticchia et al., 2014). For instance, sample should be diluted before measurements the ζ-potential and the dilution may also influence the authenticity of the system. Fotticchia et al. (2014) showed similar results by titration chitosan or poly-l-lysine into egg lecithin based emulsions and they demonstrated that ITC could provide more accurate information than DLS.

Fig. 2A showed that the enthalpy change (ΔH) in the titration was -0.534.40 kcal/mg. The Gibbs free energy (ΔG) was also negative (-8.96 kcal/mg) by fitting the curve of " one set of sites ", indicating that the interaction between the primary emulsion and LMP was a spontaneous reaction. Similar exothermic sequences were also found in ovalbumin/chitosan (Xiong et al., 2016) and soy proteins/gum Arabic (Dong et al., 2015). This result supports the generally accepted view that adsorption is primarily driven by electrostatic interactions (Burgos-Díaz et al., 2016; Fotticchia et al., 2014). Indeed, the interaction in the preparation of the multilayer emulsion is a more complex interaction than just an electrostatic mechanism. It may also include hydrophobic interactions, van-der-Waals forces, and hydrogen bonding. However, we cannot say whether these forces are present, because ITC measures the sum of all events that occur in the reaction cell. Furthermore, comparing the ΔG value (-8.13 kcal/mg) obtained from the interaction between CAS and LMP (Wang et al., 2019), it was found that the absolute value of ΔG is higher in this study. This could be attributed to the fact that the adsorbed casein (+32.6 mV) exhibited stronger surface charge than free casein molecules (+20 mV) in the continuous phase at pH 3.0 (Wang et al., 2018).

ITC measurements by titrating LMP solution into primary emulsions were also performed to understand the heat flow (Fig. 2B) in the presence of insufficient polysaccharides. Instead of decreasing regularly, the heat released of each injection increased in the initial phase and the maximum heating was obtained at ratio 0.3. Several possibilities may explain this behavior: (i) insoluble flocs were clearly observed by titration of LMP into the primary emulsion at the initial stage, and these flocs did not disappear with the continuous addition of LMP (Data not shown). This can be attributed to the bridging flocculation caused by negatively charged pectin molecules and positively charged droplets. The bridging flocculation process may be accompanied by more complex reactions than electrostatic adsorption, such as some endothermic effects (unfavorable conformational changes, hydrophobic interactions, etc. (Bou-Abdallah & Terpstra, 2012)) and, (ii) when the pH of stock solution was adjusted to 3.0 by HCl, some ions remained in the solution may inhibit binding interactions (Xiong et al., 2017) due to the formation of an ionic screen that prevents the interaction between the two biopolymers. Interestingly, the ratio 0.3 also corresponds to the starting decrease of ζ-potential (Fig. 1B), suggesting that the overall droplet surface charge in this system changed. After this ratio, the heat released after each injection started to decrease regularly and reaches the "0" point at ratio 0.7. However, Fig. 1B showed that the ζ-potential reached a plateau until the ratio 1.5, while ITC data indicated that there was no obvious heat changed at ratios higher than 0.7. This finding suggested that the continued decreased in potential caused by the addition of LMP is probably not accompanied by a significant thermal change.

3.1.3. Schematic representation of the formation of multilayer emulsions by titration

Based on the above results, a schematic diagram was established to summarize the main events occurring as function of the ratio in the titration and back-titration systems (Fig. 3). For the primary emulsion titration by LMP solution, stable multilayer emulsions are successfully formed at the initial stage, which were stable to droplet flocculation. This is because each injection contains enough LMP chains to

completely cover oil droplets and gives them a negative surface charge, thereby avoiding droplet aggregation due to electrostatic repulsion. Theoretically, as the LMP in the system is gradually depleted, the injected droplets will interact with other LMP-coated droplets, causing large droplets to aggregate. In general, bridging flocculation tends to occur earlier (before the biopolymer in the continuous phase is completely depleted), which are mainly depending on the mixing methods (mixing (Liu et al., 2019) or titration (Zeeb et al., 2015)) and biopolymer properties (e.g., charge density, molecular weight, and conformation (Gharsallaoui et al., 2010)). For back-titration, bridging flocculation occurs at the initial stage, as the injected negatively charged LMP molecules will adsorb to the surface of multiple droplets and link them together. Although negatively charged pectin continued to be added to the system, making the surface of the entire system negatively charged (Fig. 1B), the flocs that had produced did not disappear. This finding is consistent with some other reports (Liu et al., 2019; Surh et al., 2006). Clusters of droplets held together by protein bridges is generally not reversible, which can be disrupted only by strong shear forces (e.g. a second-stage of homogenization) (Dickinson, 2019). For instance, F. Liu et al (2016) mixed primary emulsions and lactoferrin and then used a blender and high pressure homogenizer to redisperse droplets to obtain stable multilayer emulsions. However, Fotticchia et al. (2014) indicated that stable multilayer emulsions can be prepared by titrating chitosan or poly-L-lysine into the primary emulsion, although bridging flocculation occurs at the initial stage of titration. Tang et al. (2021) successfully prepared multilayer emulsions by direct mixing relatively high content of sodium alginate with chitosan based picking emulsions. These differences may originate from the properties of different biopolymers (e.g., charge density, molecular weight and conformation), the primary layer thickness of emulsion droplets, as well as solution conditions (e.g., pH, ionic strength, temperature, and stirring) (Burgos-Díaz et al., 2016).

3.1.4. Analysis of fluoresence intensity

Several studies have reported (Acharya et al., 2013; Qiu et al., 2015) that CAS or CAS-based droplets exhibited an obvious emission band around 330 nm when the

extraction band was 280 nm due to the presence of tryptophan. For this reason, measurements of tryptophan fluorescence spectroscopy during the formation of CAS-LMP based multilayer emulsion were used to study CAS conformational changes, owing to the fact that the intrinsic fluorescence of tryptophan residues is highly sensitive to the polarity of microenvironments (Li et al., 2021).

Fig. 4A shows the fluorescence spectra of multilayer emulsions prepared by titrating the primary emulsion into LMP solution with different ratios and all samples maintained the same CAS content. All samples emulsion showed strong fluorescence emission upon excitation at 280 nm, with a peak near 330 nm. Interestingly, when the ratio $\leq$ 0.6, there was no obvious shift in the maximum emission wavelength of LMP-CAS based emulsion; however, when the ratio was above 0.6, the wavelength corresponding to the maximum showed a slight red shift compared to the primary emulsion. It has been reported that the red or blue shift in the emission band of CAS was usually related to changes in the tryptophan environment (Li et al., 2019). Therefore, no shift was observed at ratio $\leq$ 0.6 which suggest that binding of LMP and CAS-coated droplets in this stage did not change the tryptophan environment.

The quenching of the fluorescence intensity has been reported as an indicator of the interaction of the components in the solution (Wang et al., 2015). Therefore, the adsorption force of LMP to the surface droplets of the primary emulsion can be deduced from the test results. In this regard, the maximum fluorescence intensities of these emulsions prepared by titration as a function of ratio are plotted in Fig. 4B. In the ratio range of 0 to 0.6, titration-prepared samples showed similar maximum fluorescence intensities; however, when the ratio is greater than 0.6, the maximum intensity of samples decreases obviously with the increase of the ratio until it reaches 1.75. The decrease in entropy intensity indicates that some of the tryptophan residues of CAS adsorbed on the oil droplets were transferred from the polar surface to the hydrophobic interior, which may be due to the interaction of tryptophan located in the hydrophobic region of the protein with pectin through hydrophobic bonds. The decrease in intensity suggests that some of the tryptophan residues of CAS adsorbed on the oil droplet are transferred from the polar surface to the hydrophobic interior,

which was probably attributed to the droplet aggregation. Similar behavior was reported for aggregation of soybean protein isolate/pectin complexes (Li et al., 2021). This result also indicates that formation mechanism of multilayer emulsions by LMP and CAS coated droplet is not only electrostatic but also accompanied by a certain degree of hydrophobic interactions (especially when the droplets are extensively aggregated), which was supported by the data of ITC results. At the same time, the maximum fluorescence intensity of these samples increased as the ratio increased from 1.75 to 2.5. This can be attributed to the presence of some individual CAS-coated droplets in the system due to the relatively high CAS-based emulsion/LMP ratio.

3.2. Effect of titration or mixing on the properties of multilayer emulsions: analysis of droplet size and flocculation

It should be noted that many papers demonstrated the successful preparation of multilayer emulsions by adding primary emulsions to other coating materials (Burgos-Díaz et al., 2016; Liu et al., 2019; Shi et al., 2021). However, there are no details on how to define "add". In fact, there are many ways of addition, such as slow/quick addition, titration or direct pouring, and these different ways of addition seem to have a significant effect on droplet aggregation in the preparation of multilayer emulsions. In this section, the direct mixing and titration under stirring were used to prepare multilayer emulsions in different ratios of CAS-based emulsion/LMP. Then, dynamic light scattering (DLS) (Fig. 5A-D), creaming index (Fig. 6A), and optical microscopy (Fig.6 B) will be presented to evaluate the surface charge, mean particle size and droplet aggregation of these emulsions.

Fig.5A exhibited the zeta potential of emulsions in both preparation methods. Interestingly, the multilayer emulsions in both methods showed similar trends in surface charge as a function of ratio, although distinct flocs were observed earlier in the emulsions prepared by direct mixing. This might be the limitation of microelectrophoresis mobility method: samples need to be highly diluted and this process may have changed the surface charge of the system (Hu et al., 2017; Salvia-Trujillo et al., 2013). For example, droplet aggregation in highly concentrated

445 emulsions may be partially redispersed to some extent after dilution and agitation.
446 Primary emulsions exhibited nanoscale diameter (~300 nm, Fig. 5B) with relatively
447 lower polydispersity index (PdI) values (Fig. 5C). As the ratio increases, all emulsions
448 showed increased droplet size and PdI values, which can be attributed to the fact that
449 negatively charged LMP adsorbed on the surface of CAS-coated droplets or droplet
450 aggregates. A similar result was found in the study of chitosan/pectin-stabilized
451 multilayer emulsions (Liu et al., 2019). It is worth noting that the particle size and PdI
452 values of samples prepared by mixing method are higher than those prepared by
453 titration one. Until the ratio reached 0.8, the titration-prepared multilayer emulsions
454 still exhibited nanoscale average droplet diameter (~600 nm) based on DLS analysis;
455 however, when the ratio was higher than 0.5, the size of sample prepared by mixing
456 was outside the measurement range of DLS. This was probably attributed the fact that
457 directly mixing provides more droplets in the same time than titration, and
458 consequently droplet–droplet collisions may occur more rapidly than polyelectrolyte
459 molecules adsorb to the droplet surfaces, thereby caused larger droplets (Guzey &
460 McClements, 2006). However, during the titration process, a small number of droplets
461 added each time can be quickly encapsulated by the polyelectrolyte at a lower
462 concentration ratio. As a result, once the surface charge reached a certain value, there
463 will be a strong electrostatic repulsion between the surface and similarly charged
464 polyelectrolytes in the aqueous phase, which limits further adsorption of the
465 polyelectrolyte, thereby reducing the probability of droplet-droplet collision and
466 retarding the occurrence of particle aggregation. This result was also confirmed by the
467 droplet size distribution. The titration-prepared samples did not show distinct peaks in
468 the larger size range until ratio reached 0.5, while even with a ratio of only 0.1 (Fig.
469 5D), distinct peaks in the larger size range were detected in the sample formed by
470 mixing (Fig. 5E). This result proved that droplet flocculation is readily to occur in the
471 mixing directly methods, indicating that different adding methods have a significant
472 effect on the droplet flocculation during the formulation of multilayer emulsions.
473 Fig. 6 A showed the visual appearance of multilayer emulsions prepared by
474 directly mixing and titration methods. As expected, those prepared by mixing showed

a cream layer when the ratio increased. Even at a ratio of 0.1, a phase separation can be observed where an opaque cream layer at the top and a strongly turbid droplet-depleted layer at the bottom, which was consistent with result of particle size (Fig. 5E). This behavior can be attributed to bridging flocculation promotion leading to an increase in particle size, which facilitates gravitational separation (Grundy et al., 2018). However, when the ratio was increased to 0.5, there was a slight creaming at the bottom of the emulsion prepared by mixing, which may be due to an increase in viscosity (polymer entanglement or viscoelastic network formation) (Grundy et al., 2018). As a result, the increased viscosity restricts the upward movement of the aggregated droplets. Notably, the multilayer emulsion prepared by titration showed much better stable creaming stability than that prepared by mixing, since no obvious phase separation occurred until the ratio reached 1.0. This could be attributed to relatively low PdI value (Fig. 5C) in these emulsions.

For further analysis, the microstructure of the primary emulsion (control) and several selected multilayer emulsions prepared by titration in different ratios (0.5:1; 0.8:1; 1:1; 1.5:1; 2:1) were observed by optic microscopy. These samples represent different states of droplets during the preparation of multilayer emulsions. Compared to the primary emulsion, the multilayer emulsion also exhibits a very homogeneous microstructure in the ratio ≤ 0.5, which supports the results of the size measurements. As the ratio increased, droplet aggregation was clearly observed at higher chitosan concentrations, especially when the ratio was higher than 1.0. This is because there are not enough LMP molecules in the system to coat the droplets, and then two or more droplets share a polysaccharide chain to form aggregates. Remarkably, both extensive droplet aggregation and significantly increased droplet size (Fig. 5B) occurred around the ratio 1.0, which corresponds to the ratio where the heat released by titration (Fig. 2A) began to decrease. These findings suggest that ITC could provide accurate information on when flocculation occurs, leading to optimal conditions for the preparation of O/W multilayer emulsions.

4. Conclusion

This study tried to explain the mechanism of the formation of multilayer

emulsions by titrating primary emulsions into coating materials. According to the obtained results, ITC measurements by titration of the primary emulsion into the coating material allow the acquisition of thermodynamic characteristics of the studied system, which are fast, accurate and informative compared to the information obtained from zeta potential measurements. ITC titration confirmed that LMP does bind CAS-coated droplets through the electrostatic forces and it was a spontaneous exothermic process ($\Delta G < 0$, $\Delta H < 0$). The binding is also accompanied by hydrophobic forces. Titration of the primary emulsion into the LMP solution resulted in a stable multilayer emulsion, while titration in the opposite direction showed obvious flocs due to bridging flocculation. Meanwhile, more uniform and smaller-sized droplets can be prepared by titrating the primary emulsion into LMP solution rather than mixing them directly, which can be attributed to the fact that slow addition can effectively avoid the aggregation of droplets. Based on emulsion stability and microscopy observations, ITC appears to have the ability to define when flocculation begins, thus providing optimal conditions for the preparation of O/W multilayer emulsions. In this way, the remaining coating materials in the continuous phase of the prepared double-layer emulsion can be reduced, so as to further prepare emulsions with three or four interfaces…, thus providing more possibilities for O/W food emulsion products.

ACKNOWLEDGEMENTS

Wei Liao greatly thanks Chinese Scholarship Council for support.

CONFLICTS OF INTEREST

The author declares that there is no conflict of interest that could be perceived as prejudicing the impartiality of the research reported.

References

Acharya, D. P., Sanguansri, L., & Augustin, M. A. (2013). Binding of resveratrol with sodium caseinate in aqueous solutions. *Food Chemistry*, *141*(2), 1050–1054.

Bou-Abdallah, F., & Terpstra, T. R. (2012). The thermodynamic and binding properties of the transferrins as studied by isothermal titration calorimetry. *Biochimica et Biophysica Acta (BBA)-General Subjects*, *1820*(3), 318–325.

Bouyer, E., Mekhloufi, G., Rosilio, V., Grossiord, J.-L., & Agnely, F. (2012). Proteins, polysaccharides, and their complexes used as stabilizers for emulsions: Alternatives to synthetic surfactants in the pharmaceutical field? *International Journal of Pharmaceutics*, *436*(1), 359–378.

Burgos-Díaz, C., Wandersleben, T., Marqués, A. M., & Rubilar, M. (2016). Multilayer emulsions stabilized by vegetable proteins and polysaccharides. *Current Opinion in Colloid & Interface Science*, *25*, 51–57.

Chang, P. G., Gupta, R., Timilsena, Y. P., & Adhikari, B. (2016). Optimisation of the complex coacervation between canola protein isolate and chitosan. *Journal of Food Engineering*, *191*, 58–66.

Chang, Y., Hu, Y., & McClements, D. J. (2016). Competitive adsorption and displacement of anionic polysaccharides (fucoidan and gum arabic) on the surface of protein-coated lipid droplets. *Food Hydrocolloids*, *52*, 820–826.

Dammak, I., Sobral, P. J. do A., Aquino, A., Neves, M. A. das, & Conte- Junior, C. A. (2020). Nanoemulsions: Using emulsifiers from natural sources replacing synthetic ones—A review. *Comprehensive Reviews in Food Science and Food Safety*, *19*(5), 2721–2746.

Dickinson, E. (2019). Strategies to control and inhibit the flocculation of protein-stabilized oil-in-water emulsions. *Food Hydrocolloids*, *96*, 209–223.

Dong, D., Li, X., Hua, Y., Chen, Y., Kong, X., Zhang, C., & Wang, Q. (2015). Mutual titration of soy proteins and gum arabic and the complexing behavior studied

by isothermal titration calorimetry, turbidity and ternary phase boundaries. *Food Hydrocolloids*, *46*, 28–36.

Fotticchia, I., Fotticchia, T., Mattia, C. A., Netti, P. A., Vecchione, R., & Giancola, C. (2014). Thermodynamic Signature of Secondary Nano-emulsion Formation by Isothermal Titration Calorimetry. *Langmuir*, *30*(48), 14427–14433.

Gharsallaoui, A., Saurel, R., Chambin, O., Cases, E., Voilley, A., & Cayot, P. (2010). Utilisation of pectin coating to enhance spray-dry stability of pea protein-stabilised oil-in-water emulsions. *Food Chemistry*, *122*(2), 447–454.

Grundy, M. M. L., McClements, D. J., Ballance, S., & Wilde, P. J. (2018). Influence of oat components on lipid digestion using an in vitro model: Impact of viscosity and depletion flocculation mechanism. *Food Hydrocolloids*, *83*, 253–264.

Guzey, D., & McClements, D. J. (2006). Formation, stability and properties of multilayer emulsions for application in the food industry. *In Honor of Professor Nissim Garti's 60th Birthday*, *128–130*, 227–248.

Hu, Y.-T., Ting, Y., Hu, J.-Y., & Hsieh, S.-C. (2017). Techniques and methods to study functional characteristics of emulsion systems. *Dietary Natural Compounds*, *25*(1), 16–26.

Jafari, S. M., He, Y., & Bhandari, B. (2007). Production of sub-micron emulsions by ultrasound and microfluidization techniques. *Journal of Food Engineering*, *82*(4), 478–488.

Kim, W., Wang, Y., & Selomulya, C. (2020). Dairy and plant proteins as natural food emulsifiers. *Trends in Food Science & Technology*, *105*, 261–272.

Li, F., Wang, H., & Mei, X. (2021). Preparation and characterization of phytosterol-loaded microcapsules based on the complex coacervation. *Journal of Food Engineering*, *311*, 110728.

Li, X., Wu, G., Qi, X., Zhang, H., Wang, L., & Qian, H. (2019). Physicochemical

properties of stable multilayer nanoemulsion prepared via the spontaneously-ordered adsorption of short and long chains. *Food Chemistry*, *274*, 620–628.

Liao, W., Gharsallaoui, A., Dumas, E., Ghnimi, S., & Elaissari, A. (2021). Effect of carrier oil on the properties of sodium caseinate stabilized O/W nanoemulsions containing Trans-cinnamaldehyde. *LWT*, *146*, 111655.

Lieberman, H., Rieger, M., & Banker, G. S. (2020). *Pharmaceutical dosage forms: Disperse systems*. CRC Press.

Liu, C., Tan, Y., Xu, Y., McCleiments, D. J., & Wang, D. (2019). Formation, characterization, and application of chitosan/pectin-stabilized multilayer emulsions as astaxanthin delivery systems. *International Journal of Biological Macromolecules*, *140*, 985–997.

Liu, F., Wang, D., Sun, C., McClements, D. J., & Gao, Y. (2016). Utilization of interfacial engineering to improve physicochemical stability of β-carotene emulsions: Multilayer coatings formed using protein and protein–polyphenol conjugates. *Food Chemistry*, *205*, 129–139.

Liu, G., Hu, M., Du, X., Qi, B., Lu, K., Zhou, S., Xie, F., & Li, Y. (2022). Study on the interaction between succinylated soy protein isolate and chitosan and its utilization in the development of oil-in-water bilayer emulsions. *Food Hydrocolloids*, *124*, 107309.

McClements, D. J. (2012). Advances in fabrication of emulsions with enhanced functionality using structural design principles. *Current Opinion in Colloid & Interface Science*, *17*(5), 235–245.

Mundo, J. L. M., Zhou, H., Tan, Y., Liu, J., & McClements, D. J. (2021). Enhancing emulsion functionality using multilayer technology: Coating lipid droplets with saponin-polypeptide-polysaccharide layers by electrostatic deposition. *Food Research International*, *140*, 109864.

610 Ogawa, S., Decker, E. A., & McClements, D. J. (2003). Production and
611 characterization of O/W emulsions containing cationic droplets stabilized by
612 lecithin− chitosan membranes. *Journal of Agricultural and Food Chemistry*,
613 *51*(9), 2806–2812.

614 Ogawa, S., Decker, E. A., & McClements, D. J. (2004). Production and
615 characterization of o/w emulsions containing droplets stabilized by lecithin−
616 chitosan− pectin mutilayered membranes. *Journal of Agricultural and Food*
617 *Chemistry*, *52*(11), 3595–3600.

618 Okubo, T., & Suda, M. (2003). Multilayered adsorption of macrocations and
619 macroanions on colloidal spheres as studied by dynamic light scattering
620 measurements. *Colloid and Polymer Science*, *281*(8), 782–787.

621 Qiu, C., Zhao, M., Decker, E. A., & McClements, D. J. (2015). Influence of protein
622 type on oxidation and digestibility of fish oil-in-water emulsions: Gliadin,
623 caseinate, and whey protein. *Food Chemistry*, *175*, 249–257.

624 Salvia-Trujillo, L., Qian, C., Martín-Belloso, O., & McClements, D. J. (2013).
625 Influence of particle size on lipid digestion and β-carotene bioaccessibility in
626 emulsions and nanoemulsions. *Food Chemistry*, *141*(2), 1472–1480.

627 Shi, F., Tian, X., McClements, D. J., Chang, Y., Shen, J., & Xue, C. (2021). Influence
628 of molecular weight of an anionic marine polysaccharide (sulfated fucan) on
629 the stability and digestibility of multilayer emulsions: Establishment of
630 structure-function relationships. *Food Hydrocolloids*, *113*, 106418.

631 Surh, J., Decker, E. A., & McClements, D. J. (2006). Influence of pH and pectin type
632 on properties and stability of sodium-caseinate stabilized oil-in-water
633 emulsions. *Food Hydrocolloids*, *20*(5), 607–618.

634 Tang, Y., Gao, C., Zhang, Y., & Tang, X. (2021). The microstructure and
635 physiochemical stability of Pickering emulsions stabilized by chitosan
636 particles coating with sodium alginate: Influence of the ratio between chitosan
637 and sodium alginate. *International Journal of Biological Macromolecules*, *183*,

1402–1409.

Wang, J., Dumas, E., & Gharsallaoui, A. (2019). Low Methoxyl pectin / sodium caseinate complexing behavior studied by isothermal titration calorimetry. *Food Hydrocolloids*, *88*, 163–169.

Wang, J., Souihi, S., Amara, C. B., Dumas, E., & Gharsallaoui, A. (2018). Influence of low methoxyl pectin on the physicochemical properties of sodium caseinate- stabilized emulsions. *Journal of Food Process Engineering*, *41*(8), e12906.

Wang, X., Liu, F., Liu, L., Wei, Z., Yuan, F., & Gao, Y. (2015). Physicochemical characterisation of β-carotene emulsion stabilised by covalent complexes of α-lactalbumin with (−)-epigallocatechin gallate or chlorogenic acid. *Food Chemistry*, *173*, 564–568.

Xiong, W., Ren, C., Jin, W., Tian, J., Wang, Y., Shah, B. R., Li, J., & Li, B. (2016). Ovalbumin-chitosan complex coacervation: Phase behavior, thermodynamic and rheological properties. *Food Hydrocolloids*, *61*, 895–902.

Xiong, W., Ren, C., Tian, M., Yang, X., Li, J., & Li, B. (2017). Complex coacervation of ovalbumin-carboxymethylcellulose assessed by isothermal titration calorimeter and rheology: Effect of ionic strength and charge density of polysaccharide. *Food Hydrocolloids*, *73*, 41–50.

Zeeb, B., Lopez-Pena, C. L., Weiss, J., & McClements, D. J. (2015). Controlling lipid digestion using enzyme-induced crosslinking of biopolymer interfacial layers in multilayer emulsions. *Food Hydrocolloids*, *46*, 125–133.

Zhang, S., Tian, L., Yi, J., Zhu, Z., Decker, E. A., & McClements, D. J. (2020). Mixed plant-based emulsifiers inhibit the oxidation of proteins and lipids in walnut oil-in-water emulsions: Almond protein isolate-camellia saponin. *Food Hydrocolloids*, *109*, 106136.

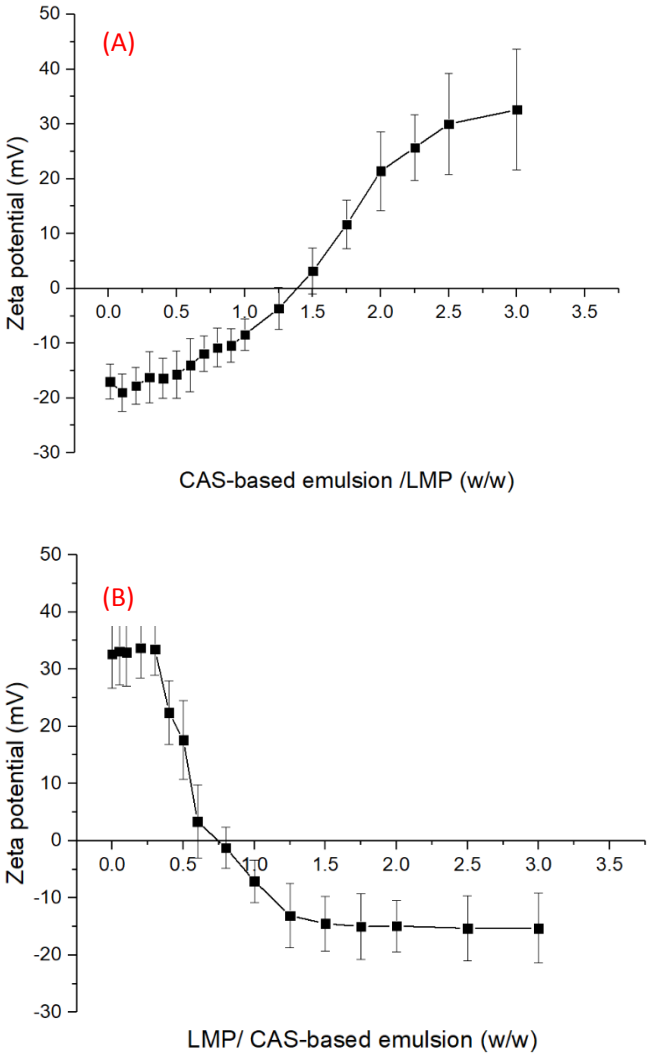

664 **Fig. 1.** ζ-potential of multilayer emulsions at pH 3.0 as a function of ratio: (A) titrating the
665 primary emulsion into LMP solution or (B) titrating LMP solution into the primary emulsion.
666
667

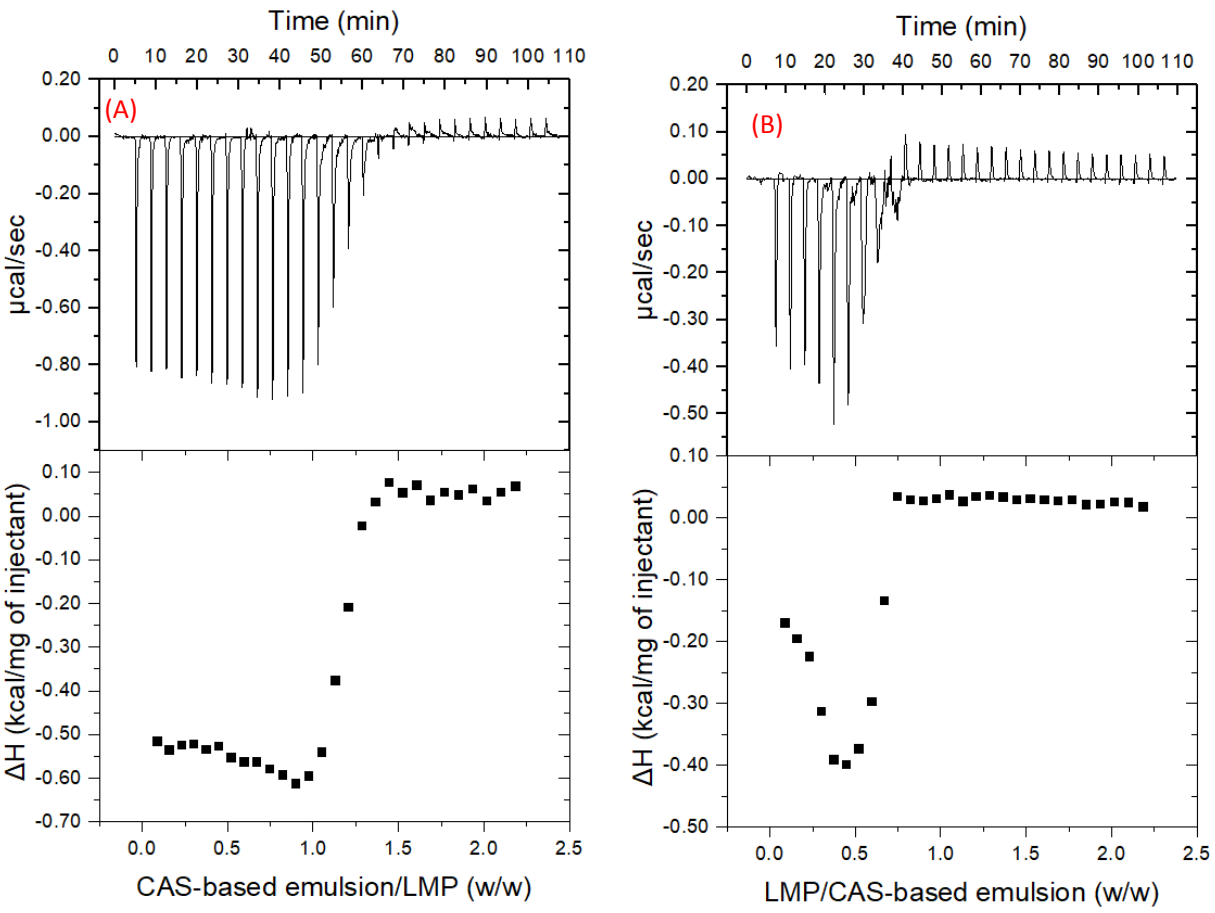

668 **Fig. 2.** ITC titration graphs (Upper) and enthalpy change (Lower) of (A) CAS-based
669 emulsion/LMP and (B) LMP/CAS-based emulsion at pH 3.0. The calorimetric cell and the syringe
670 were filled with 0.05 wt.% CAS-based emulsion and 0.5 wt.% LMP solution or 0.05 wt.% LMP
671 and 0.5 wt.% CAS-based emulsion.
672

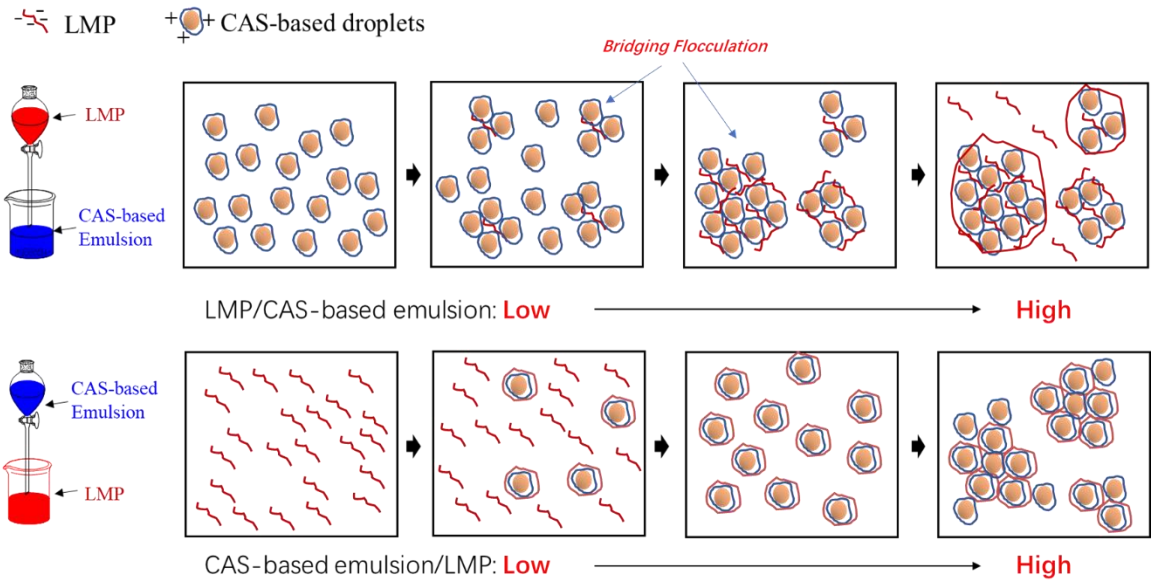

673 **Fig. 3.** Schematic representation of the formation of multilayer emulsions by titration based on
674 CAS-coated emulsion and LMP at pH 3.0.
675

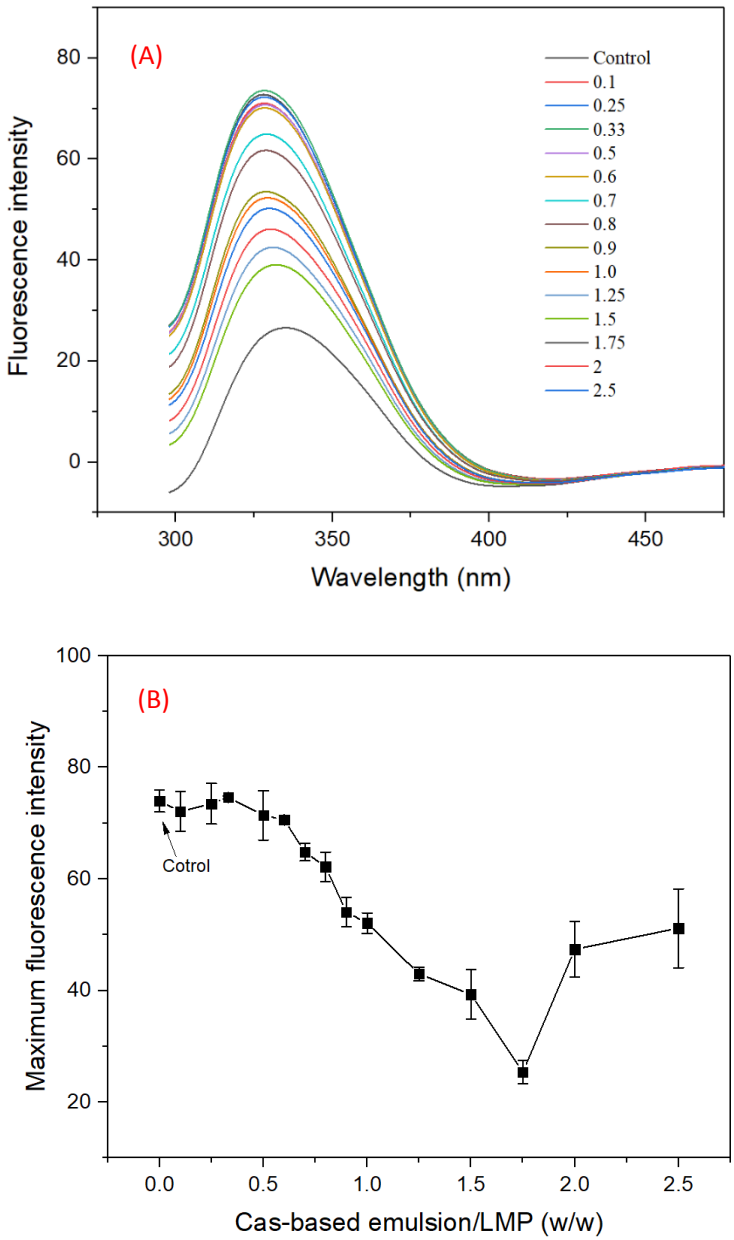

676 **Fig. 4.** (A) Fluorescence spectra and (B) maximum intensity of multilayer emulsions as a function
677 of ratio by titrating the primary emulsion into LMP solution. The excitation wavelength was set to
678 280 nm and the emission slit width was 5 nm.
679

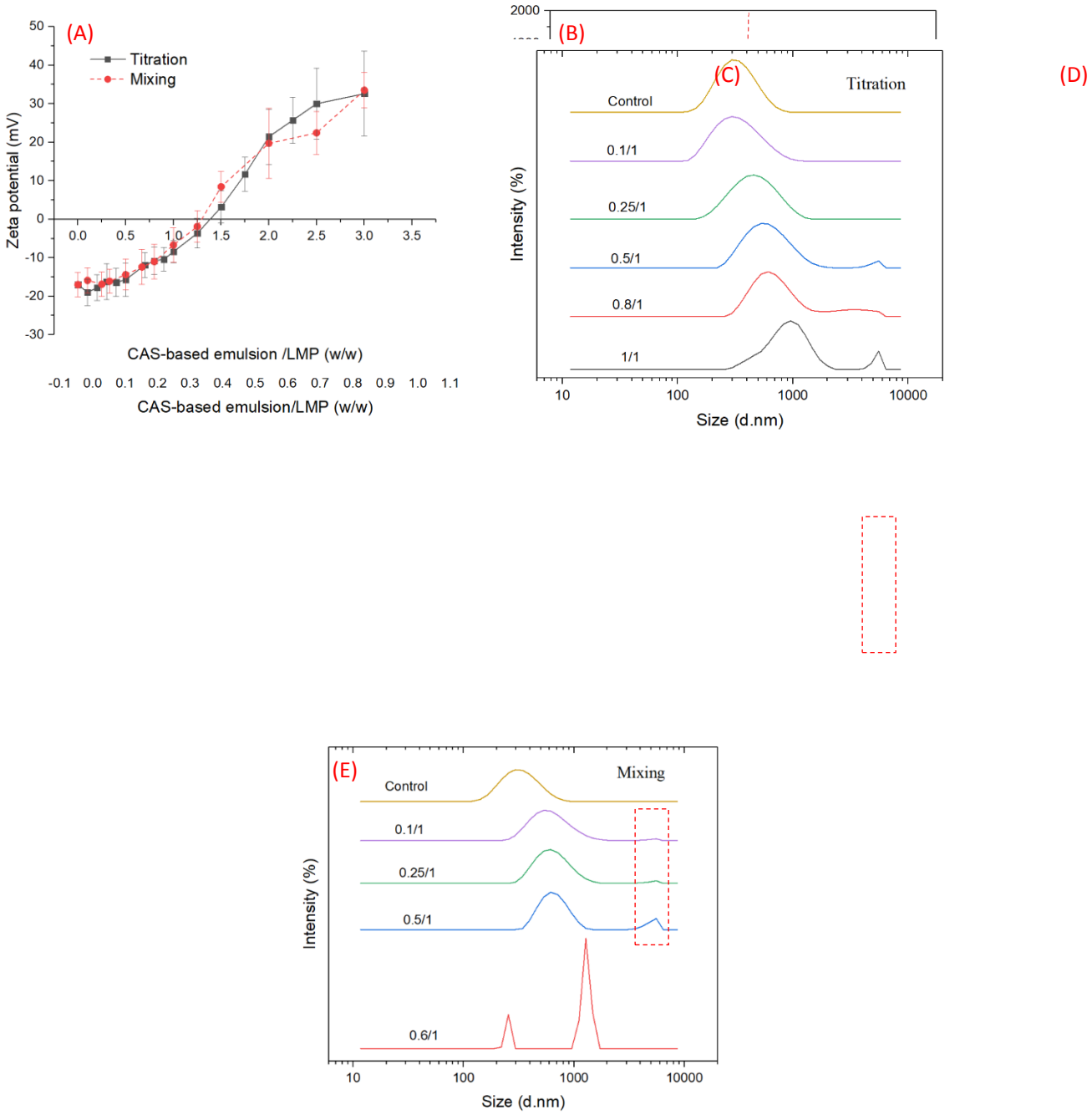

Fig. 5. (A) ζ-potential, (B) Mean particle size, and (C) Polydispersity index as a function of ratio by titrating or mixing directly based on CAS-based emulsion and LMP; The particle size distributions as function of ratio prepared by (D) titration or (E) mixing.

(A)

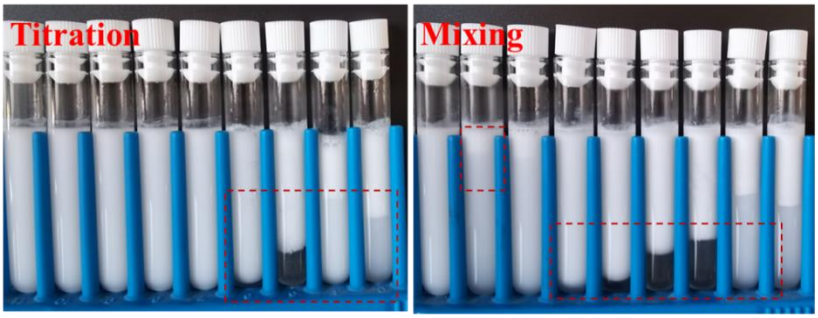

Ratio (w/w, left to right): 0 - 0.1 - 0.25 - 0.5 - 0.8 - 1.0 - 1.25 - 1.5 - 2.0

(B)

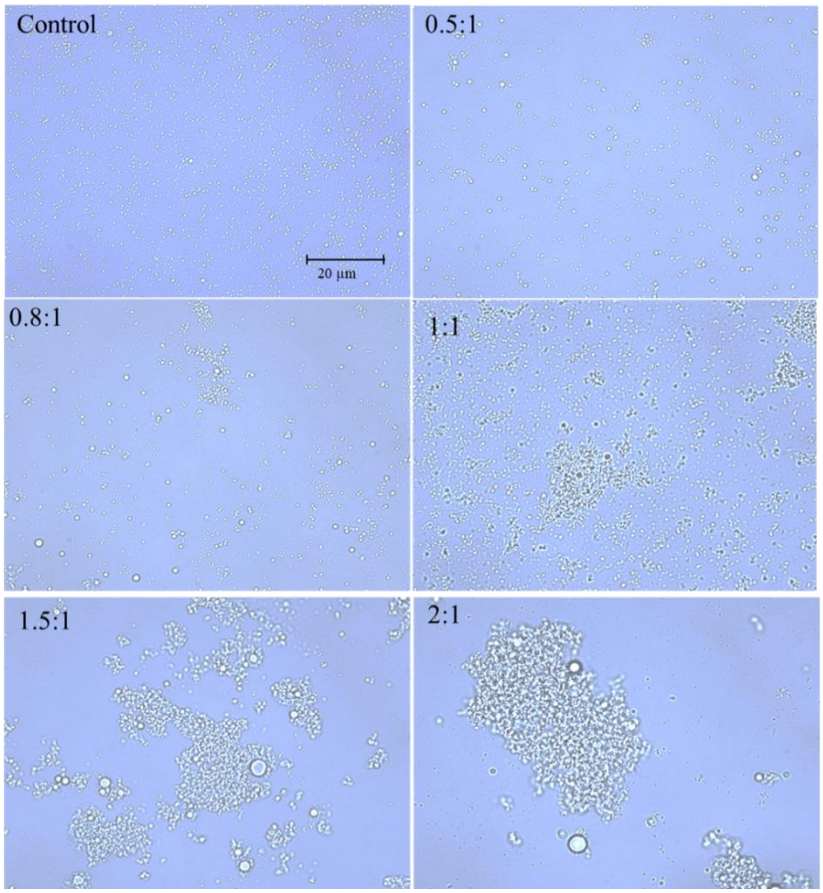

Fig. 6. (A) Visual appearance of multilayer emulsions prepared by titration or mixing as function of ratio and (B) Photomicrographs of multilayer emulsions prepared by titration. The scale bar is 20 µm in length.